Evaluation of behavior of updated three-dimensional panel under lateral load in both independent and dependent modes

Omid Rezaifar[*1], Hamun Adeli Nik[2a] and Majid Ghohaki[1b]

[1]*Department of Civil Engineering, Semnan University, Across from Sokan Park, Semnan, Iran*
[2]*Faculty of Civil Engineering, Semnan University, 18, 28 Street, Gisha, Tehran, Iran*

Abstract. Three-dimensional panels are one of the modern construction systems which can be placed in the category of industrial buildings. There have always been a lot of studies and efforts to identify the behavior of these panels and improve their capacity due to their earthquake resistance and high speed of performance. This study will provide a comparative evaluation of behavior of updated three-dimensional panel's structural components under lateral load in both independent and dependent modes. In fact, this study tries to simultaneously evaluate strengthening effect of three-dimensional panels and the effects of system state (independent, *L*-shaped and BOX shaped Walls) with reinforcement armatures with different angles on the three-dimensional panels. Overall, six independent wall model, *L*-shaped, roofed *L*-shaped, BOX-shaped walls with symmetric loading, BOX -shaped wall with asymmetrical loading and roofed BOX-shaped wall were built. Then the models are strengthened without strengthened reinforcement and with strengthened reinforcements with an angle of 30, 45 and 60 degrees. The applied lateral loading, is exerted by changing the location on the end wall. In BOX-shaped wall, in symmetric and asymmetric loading, the load bearing capacity will be increased about 200 and 50% respectively. Now, if strengthened, the load bearing capacity in symmetric and asymmetric loading will be increased 3.5 and 2 times respectively. The effective angle of placement of strengthened reinforcement in the independent wall is 45 and 60 degrees. But in BOX-shaped and *L*-shaped walls, the use of strengthened reinforcement 45 degrees is recommended.

Keywords: three-dimensional panels; independent mode and system; improvement of lateral load capacity; strengthening panel

1. Introduction

Normally, nowadays, the application of 3D panels in the construction industry has spread with the growing attention to style creation and use of prefabricated components. These systems due to their advantages over the older systems have attracted builders. But it needs more comprehensive studies since it is a new method in the construction industry. Prefabricated concrete Sandwich panels can be used as the external walls in residential buildings and tank walls. Fig. 1 shows a view of a panel showing (Bassotti and Ricci 2002). Weight loss and safety of buildings against earthquakes (about 25% by weight of the building is reduced), reduced implementation time, the transport speed and ease in height and impassable areas, sound insulation and humidity, energy saving and so on are among the advantages of these panels. This concept was introduced after the works of Kabir (2005) and the strategic supervision department of military affairs of Iran (2012) (Kabir 2005).

∗Corresponding author, Associate Professor
 E-mail: Orezayfar@semnan.ac.ir
[a]M.Sc. Graduate
 E-mail: hamun_98@yahoo.com
[b]Associate Professor
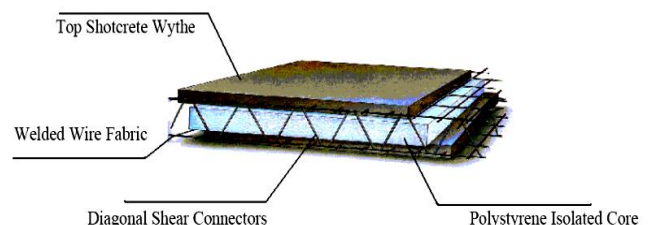 E-mail: mgholhaki@semnan.ac.ir

Fig. 1 Load bearing prefabricated wall (Rezaifar *et al.* 2008)

2. Different types of three-dimensional panels

These panels are divided into two types of wall panels and floor panels:

2.1 Specifications of wall panels

Wall panels are used as vertical Load bearing elements as well as earthquake-resistant element. Wide gravity load is distributed on each wall according to its load receptor level. The lateral load caused by the earthquake is distributed on the walls through rigid diaphragm of the floor compared to stiffness between walls. The thickness of polystyrene is 6 cm and the distance between two grids is 10 cm in these panels. Also the thickness of shot Crete concrete is 4 cm on each side of the wall. Fig. 2 shows the
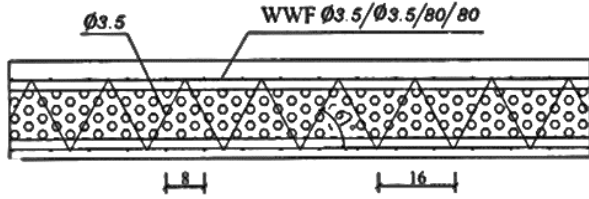
Fig. 2 Specification wall panel, longitudinal sections of the panels (strategic supervision department of military affairs Iran 2012)

specifications of wall panel. This concept was introduced after the works of strategic supervision department of military affairs of Iran (2012)

2.2 Specifications of floor panels

Wall Floor panel acts as a unilateral slabs which is due to existence of cutting components in the longitudinal direction of the panel. The thickness of the polystyrene layer based on the design of floor slab is variable between 6 and 10 cm. floor slab must be updated since the used grid has a little steel in which resistant anchor has been calculated based on the length of span and applied load and a series of additional armatures will be embedded at regular intervals in the panel.

3. History

In the technical literature several experimental campaigns on precast sandwich panels with shear connectors can be found. This concept was introduced after the works of PCI Committee (1997), Benayoune *et al.* (2006), Benayoune *et al.* (2007), Benayoune *et al.* (2008), Salmon *et al.* (1997, 1994), Bush *et al.* (1994), Kabir (2002), Giacchetti (1984). On the contrary, very few experimental tests have been performed on sandwich panels with in situ sprayed concrete and no-shear connectors, this concept was introduced after the works of Ceccoli (2002), Bassotti (2002) and on 3D full scale mock-up in order to study the behaviour of the panels in real structures by Rezaifar *et al.* (2008). Consequently, general conclusions on the structural behaviour of this construction system cannot be drawn and further experimental investigations are needed.

As regards compression tests, High ultimate loads, decreasing for increasing values of the slenderness ratios, were obtained. The numerical simulations indicated that the ultimate loads of axially loaded panels are close to the buckling loads which can be determined by performing a linear buckling analysis by using the coefficient a. Differently, the ultimate loads of eccentrically loaded panels, which are significantly lower than the buckling loads, can be simulated only by performing a non-linear analysis (Gara *et al.* 2012).

Kabir *et al.* (2007) have studied the 3D slabs. When the structural performance is concerned, the main disadvantage of 3D panel, when used as floor slab, is their brittleness in flexure. The current study focuses on upgrading ductility

and load carrying capacity of 3D slabs in two different ways; using additional tension reinforcement, and inserting a longitudinal concentrated beam (Kabir *et al.* 2007).

Numayr and Haddad (2009) have studied the structural performance of this system. To investigate the structural performance of this system, an extensive experimental testing program for ceiling and wall panels subjected to static and dynamic loadings was conducted. (Numayr and Haddad 2009).

Kabir *et al.* (2009) have studied the types of wall connection.Two different types of *L*-shaped wall connection, with and without vertical small column at the conjunction are cast. The measured values of applied load and 6 displacements are recorded by a computer data logger capable of measurement to sensitivity ranges of 0.1 N, 0.001 mm, respectively (Kabir *et al.* 2009).

Foster and Rogowsky (1997) have studied the concentrated loads on reinforced concrete panels. Two cases are examined (i) panels loaded concentrically, and (ii) panels loaded eccentrically. The numerical investigation suggests that the bursting force distribution is substantially different from that calculated using elastic design methods currently used in some codes of practice. The optimum solution for a uniformly reinforced bursting region was found to be with the reinforcement distributed from approximately 0.2 times the effective depth of the member (0.2D(e)) to between 1.2D(e) and 1.6D(e) (Foster and Rogowsky 1997). Malekzadeh (2015) have studied the cores of sandwich panels.

4. Determining the specifications of three dimensional panel structures

4.1 Determining the target displacement

One of the methods that are used to determine the target location is the method of displacement coefficients. Ease in use is among its advantages. A non-linear static analysis done is done in this method and base cutting curve is obtained against lateral displacement of control point. The target displacement can be obtained using this curve. The target displacement must be initially calculated for this method (Pekelnicky and Poland 2012)

$$\delta_t = C_0 C_1 C_2 C_3 S_a \frac{T_e^2}{4\pi^2} g \tag{1}$$

In which is T_e the effective building fundamental period, C_0 is the correction factor to correct the spectral displacement of a system with one degree of freedom to a system with displacement of a system with several degrees of freedom, C_1 is the Correction factor to convert the displacement calculated from linear elastic response to the expected maximum inelastic displacements of structure, C_2 is the correction factor to consider the shape of hysteresis curve, reduced hardness and deterioration of structural members resistance on the maximum displacements, C is the correction factor to consider the increasing displacements caused by *P*-Delta (Pekelnicky and Poland 2012).

K_i and K_e Are respectively elastic lateral stiffness and

Table 2 Caption C_2 values (Pekelnicky and Poland 2012)

The level of desired performance	$T \geq T_s$		$T \leq 0.1$	
	Type2	Type1	Type2	Type1
Uninterrupted use feature	1.00	1.00	1.00	1.00
Life safety	1.00	1.10	1.00	1.30
Verge of collapse	1.00	1.20	1.00	1.50

Fig. 3 Additional load diagram (Pekelnicky and Poland 2012)

effective lateral stiffness of the structure in thee studied order and T_i is the time of main alternation of structure with use of which T_e which is the main effective alternation of structure is calculated using the following equation (Pekelnicky and Poland 2012)

$$T_e = T_i \sqrt{\frac{K_i}{K_e}} \qquad (2)$$

Values for C_0 will be calculated using Table 1. C_1 is also calculated as follows (Pekelnicky and Poland 2012)

$$T_e \geq T_s \rightarrow C_1 = 1 \qquad (3)$$

$$T_e \prec T_s \rightarrow C_1 = \max\left[1, \frac{\left[1.0 + (R-1)\frac{T_s}{T_e}\right]}{R}\right] \qquad (4)$$

In which T_S is the common time period between two areas of constant acceleration and constant speed in reflectance spectrum of the project which is calculated based on Table 3, 2008 Regulationof Iran (2012).

Also the values for C_2 are calculated using Table 2. C_3 coefficient depends on line slope in the inelastic area. This coefficient is different for positive and negative surrender. C_3 Coefficient is equal to one for structures with hardness after positive surrender and is equal the following zero for structures with hardness after negative surrender (Pekelnicky and Poland 2012)

$$C_3 = 1.0 + \frac{|\alpha|[R-1]^{.5}}{T_e} \qquad (5)$$

Which do not need to have higher values than values calculated for C_3 in the following equation (Pekelnicky and Poland 2012)

$$C_3 = 1.0 + \frac{|\alpha|[R-1]^{.5}}{T_e} \qquad (6)$$

4.1 Determining the hardness of the structure

One of the methods that are used to determine. The hardness of the structure is calculated in two start points of the additional load diagram and at $0.6V_y$.

5. Determining the specifications of three dimensional panel structures evaluation of the performance three-dimensional panels

In the technical literature several experimental campaigns In order to evaluate the behavior of three-dimensional panel
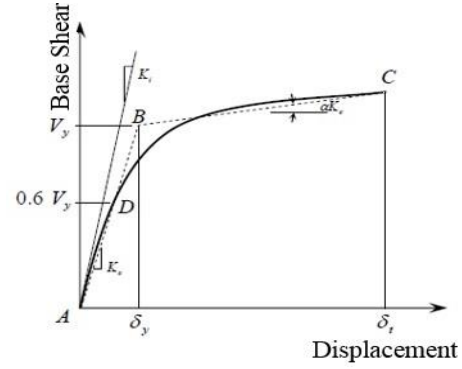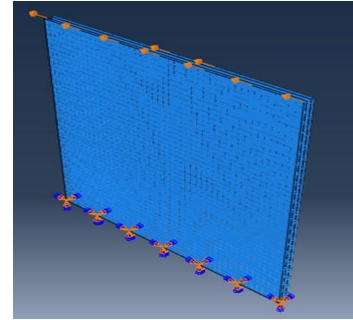

Fig. 4 Model and method of loading of independent Wall)

walls under the effect of cycles and constant loads. Also 24 wall panels with dimensions close to reality (360×360 cm) in modes of independent walls, *L*-shaped walls, *L*-shaped walls with roof, BOX shape walls with symmetric load, BOX shape walls and BOX shape walls with asymmetrical loading and BOX shape with roof that each model comes with reinforcement armature are placed under static loading in Abaqus software with angles of 30, 45 and 60 degrees to control the analytical and numerical results. This loading will be placed in form of a back and forth modal shift at the end of the wall. One side of the wall is clamped in this mode and additional load curve is drawn by gradually applying a specified displacement to the end of the wall and measurement of forces created in the wall (Fig. 4).

Created models can be divided into four main groups and each consists of six models. The first group has walls with no reinforced armatures. The second group models with 30 degrees reinforcement armatures. Also the third and fourth groups have walls with respectively 45 and 60 degrees reinforcement armatures. It should be noted that the angel of reinforcement armatures with the horizon must be considered here. Reinforcement armatures are ribbed armatures with a diameter of 10 mm. each of the groups consists of six models. Independent wall have been modeled in the first model. *L*-shaped wall without roof and *L*-shaped wall with roof have been respectively evaluated for the second and the third models. The fourth model is BOX shaped wall without roof with in influenced by a symmetrical load. Load in applied in asymmetrical form in the fifth model. The last model is BOX shaped wall with roof. It should be noted that roofs have been modeled rigidly. Table 3 shows the naming method of these models.
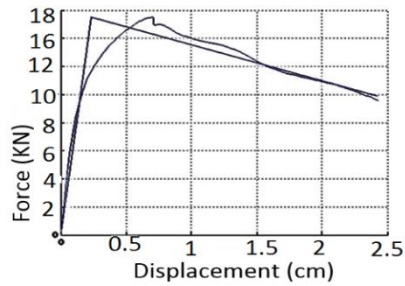
Fig. 5 Additional load curve of three-dimensional independent panel without armature

Table 3 Method of naming the models

Number of word	Sign	Explanation
The first word	I	Independent wall
(determines the shape of the wall)	L	L-shaped wall
	B	B-shaped wall
The second word	O	No roof and symmetrical load
(determines the conditions of roof and loading mode)	T	Without a roof with load asymmetrical
	R	With Roof and symmetrical load
The third word	A00	Without reinforcement armature
(determines the existence and the angle of reinforcement armature)	A30	armature reinforcement with an angle of 30 degree
	A45	armature reinforcement with an angle of 45 degree
	A60	armature reinforcement with an angle of 60 degree

Table 4 The concrete compression stress strain values

Stress (MPa)	Plastic strain	Inelastic strain	Strain
19/22	0/000741	0/00000	0/00000
27/33	0/0011405	0/00014	0/00013
33/71	0/001595	0/00037	0/00033
37/31	0/002076	0/00072	0/00064
38/44	0/0026102	0/00121	0/00107
36/79	0/003436	0/00209	0/00186
33/26	0/004324	0/00311	0/00276
29/20	0/005294	0/00423	0/00376
25/30	0/006349	0/00543	0/00484
21/92	0/00825	0/00752	0/00667
19/07	0/008623	0/00793	0/00701
16/67	0/009856	0/00925	0/00805
14/64	0/011165	0/01063	0/00891

Table 5 The concrete tensile stress strain values

Stress (MPa)	Strain	cracking strain
1/77	0/000083	0/000000
1/41	0/000104	0/000052
0/72	0/000333	0/000307
0/16	0/000724	0/000719

As it can be observed in additional load curve in Fig. 5, two line additional load curve is used to find target displacement. Also the maximum load bearing capacity in independent three-dimensional wall panels without armature strengthening is 15500. The area of additional load curve has been calculated next which its higher values will lead to absorbance of more energy from the structure. The area under the additional load curve is equal to 296 Newton-meters. Independent panel wall without opening has a great hardness due to the type of material and three-dimensional behavior and the dimensions of the sample was in way that it showed a flexural behavior. Given the weakness of concrete in tension, the cracks were primarily in stretching form caused by bending and shear cracks occurred in larger displacements and the load-shift curve has a short nonlinear area for this reason which indicates low forming factor of the panel.

Additional load curves of models have been drawn in different modes together for qualitative comparison between panels and then the maximum load bearing capacity and energy absorption of the structure have been qualitatively compared with each other.

In numerical method, it was tried to make the software model consistent with reality. The welded grid in all samples was composed of wires with diameters of 3.5 mm, vertically and horizontally located with distance of 80 mm and also of wires with diameter of 3.5 mm with the same kind of the grid wires. Also, the diameter of reinforcement armature is 10 mm. The thickness of the insulation layer in all samples is 60 mm and made of polystyrene and the

thickness of spraying concrete in each side of the samples was about 4-5 cm. One end of the wall is connected to the clamp support and side load is applied to its other end. The method of loading is in the form of displacement applied on the end of the wall.

The Solid element has been used for meshing. The meshing dimensions are 8×8. For concrete modelling, the eight-node element, Solid C3D8 has been used in which the dimensions of each mesh for the element are 8×8 cm^2. For bar modelling, two-node element of B31 Beam has been used. The bars have been connected to the concrete by using Embedded Regions Technique. Furthermore, the Concrete compression stress strain values were obtained according to Table 4 and the Concrete tensile stress strain values were obtained according to Table 5. It can be said that due to the low strength of polystyrene in comparison with concrete and steel, the polystyrene strength in software has been ignored.

A-concrete: for concrete modelling, the SOLID element was used. In numerical modelling it was tried to make inputs of ABAQUS program based on the results related to the specifications of the component constituent panel. To define the specifications of shot Crete concrete in software, the damaged concrete elasticity modulus has been used. This model has been a continuous model based on the plasticity which has the ability to analyze concrete structures and model damage in concrete. In this study, the considered mechanical specifications in damaged elasticity of concrete have been presented in Table 6.

About the elasticity modulus of shot Crete concrete it should be said that its value does not obtain from the relation given in concrete regulations of Iran, i.e., $E_c = 5000\sqrt{f_c'}$. According to previous studies, the elasticity modulus value of shot Crete has been suggested as 0.25 to

Table 6 Mechanical specifications of shot Crete concrete

Specific mass Kg/m^3	Elasticity (GPa)	Poisson ratio	Concrete strength (MPa)	Concrete tensile strength (MPa)
2350	3-15	0.15	16	1-2.5

Table 7 Mechanical specifications of steel (grid and reinforced)

The type of steel	Poisson's ratio	Specific weight Kg/m^3	Elasticity modulus (GPa)	Yield stress (MPa)	Ultimate stress (MPa)
grid	0.3	7855	210	450	570
reinforced	0.3	7855	210	300	500

0.5 of the obtained value from the expression above. In this study, regarding the specific compressive strength, 0.3 of the value obtained from the expression above, has been the modelling criterion.

B-steel: to introduce the specifications of this structure in software, the two-line elasto-plastic model has been used. The mechanical specifications of steel have been considered according to Table 7.

5.1 Verification of software model

Tested panels were modeled using (Abaqus) software and the same displacements applied in experimental method have been defined for the modeled panels. Applying support and load conditions is in a way that one end of the wall is connected to clamped support and side load is applied to its other end. The method of loading is in form of displacement applied on the end of the wall. The validation of thee modeling is evaluated with comparison of force-shift curve obtained from numerical analysis of finite element model using Abaqus software with Jahanpour-Kabir experimental model (Kabir *et al* 2004, Kabir and Vasheghani-Farahani 2009). According to Fig. 6 (Dotted line: experimental model, continuous line: software version) it can be observed that the created model has an acceptable accuracy (Kabir *et al.* 2004).
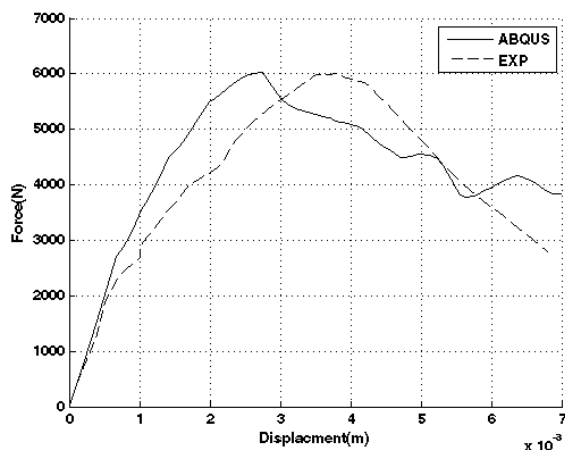

Fig. 6 Force-shift curve obtained from numerical analysis of finite element model
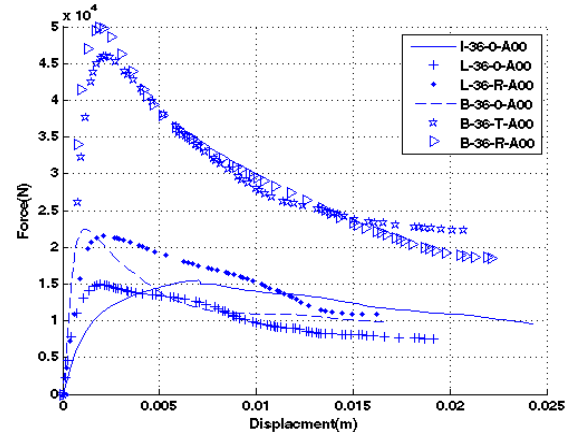

Fig. 7 Compressive additional load curve of panel without reinforcement armature

Table 8 The comparison of panel's quantitative results in six modes without reinforcement armature

Row	model's name	The maximum load capacity (N)	Percent of increased bearing capacity	Energy absorption of the structures (N.m)	Percent of increased absorption Energy in the structure
1	I-O-A00	15.500	0%	296	0%
2	L-O-A00	14.916	-4%	199	-33%
3	L-R-A00	21.572	39%	253	-15%
4	B-O-A00	46.015	197%	610	106%
5	B-T-A00	22.480	45%	215	-27%
6	B-R-A00	49.886	222%	647	119%

5.2 Panel without reinforcement armature

Fig. 7 shows the additional load curve of Panel without reinforcement armature in six mentioned models. First, maximum load capacity and energy absorption are measured for each model. Then increase percentage of load bearing and increase percentage of energy absorption have been calculated compared to the independent wall. These values have been mentioned in Table 8.

According to Fig. 7 and Table 8, it can be concluded that connecting two panel walls in *L*-shape without roof and without reinforcement armature , not only will not increase the structural strength but Wall resistance will be reduced due to the emergence of twists in the structure. Although by adding a roof to the system, lateral load capacity will increase by as much as 39%, it should be noted that the reason for this increased resistance is the dramatic reduction of twisting effect of the structure. The lateral load capacity of will be nearly three times larger than an independent wall in box shaped mode. However, this increased load bearing will be 100% if asymmetric loading causes a twist in structure in BOX shape mode. It is noteworthy that adding roof to the panels will only add 10% to the capacity compared to symmetrical load without a roof. It can be suggested according to this theorem that creating BOX shape mode can significantly improve lateral load bearing capacity if there is the possibility to remove twists caused by symmetric load from the structure.
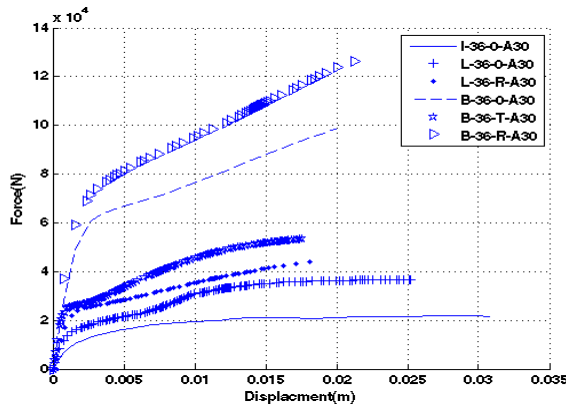
Fig. 8 Lateral additional load curve with panel with 30 degrees reinforcement armature reinforcement armature

Table 9 The comparison of panel's quantitative results in six modes with 30 degrees reinforcement armature

Row	Model's name	The maximum load capacity (N)	Percent of increased bearing capacity	Energy absorption of the structures (N.m)	Percent of increased absorption Energy in the structure
1	I-O-A30	21.930	0%	587	0%
2	L-O-A30	36.829	68%	745	27%
3	L-R-A30	44.002	101%	597	2%
4	B-O-A30	98.526	349%	1,483	153%
5	B-T-A30	53.334	143%	711	21%
6	B-R-A30	126.440	477%	1,991	239%

5.3 Panel with 30 degrees reinforcement armature

Fig. 8 shows the additional load comparative curve of Panel with 30 degrees reinforcement armature in 6 mentioned modes.

The maximum lateral load capacity and energy absorption have been initially calculated for each model. Then, increase percentages of load capacity and energy absorption have been calculated compared to the independent wall. These values have been mentioned in Table 9.

It can be concluded according to Fig. 8 and Table 9 that unlike panels without reinforcement armature, connecting 2 panel wall to each other in *L*-shaped mode without roof but with 30 degrees reinforcement armature will increase the bearing capacity of the structure. This model properly shows the effect of reinforcement armature. In a way that the existence of reinforcement armature will make the wall to have bearing against twisting load. Now the lateral load bearing capacity will be 2 times bigger by adding roof to this system which properly shows the effective effect of reinforced armature.

The lateral load bearing capacity of the wall will be 4.5 times bigger than an independent wall in BOX shape mode. This increased load bearing capacity will even be 2.5 times bigger in BOX shape loading with asymmetric loading which will lead to creation of twist in the structure. It is noteworthy that adding roof to the panels will make the load bearing capacity to be 6 times bigger. It can be suggested
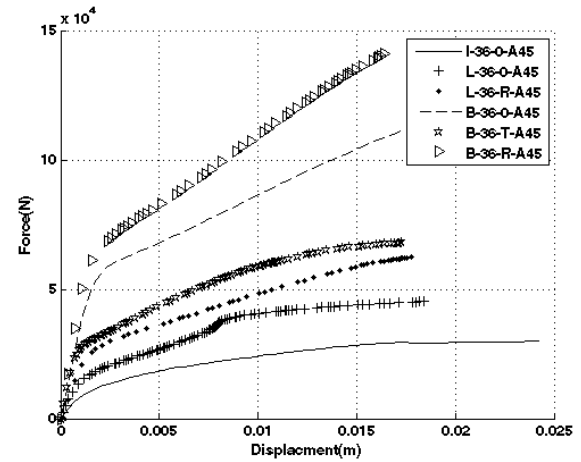

Fig. 9 The comparative additional load curve of panel with 45 degree reinforced armature

Table 10 The comparison of panel's quantitative results in six modes with 45 degrees reinforcement armature

Row	Model's name	The maximum load capacity (N)	Percent of increased bearing capacity	Energy absorption of the structures (N.m)	Percent of increased absorption Energy in the structure
1	I-O-A45	29,500	0%	573	0%
2	L-O-A45	45,332	54%	632	10%
3	L-R-A45	62,331	111%	780	36%
4	B-O-A45	110,987	276%	1,359	137%
5	B-T-A45	68,001	131%	887	55%
6	B-R-A45	140,858	377%	1,587	177%

according to this theorem that creating BOX shape mode can significantly improve lateral load bearing capacity if there is no possibility to remove twists caused by symmetric load from the structure.

5.4 Panel with 45 degrees reinforcement armature

Fig. 9 shows the additional load comparative curve of Panel with 45 degrees reinforcement armature in 6 mentioned modes. The maximum lateral load capacity and energy absorption have been initially calculated for each model. Then, increase percentages of load capacity and energy absorption have been calculated compared to the independent wall. These values have been mentioned in Table 10.

It can be concluded that similar to 30 degrees reinforcement armatures, 45 degrees reinforcement armatures will properly improve the performance of the panel influenced by the applied twist and allows the structure to act under the effect of the system which means as same as Table 10, *L*-shaped system will lead to 54% improvement and *L*-shaped system with roof will lead to 111% improvement. It is noteworthy that energy absorption of the structure will increase under *L*-shape performance, even though this increase will be about 10 to 30 percent.

The lateral load capacity of the wall will increase by 276% compared to an independent wall. Also in BOX shape
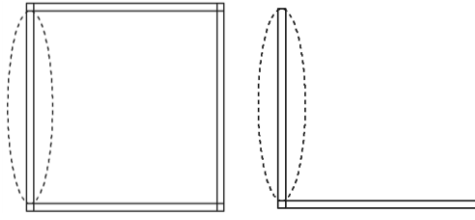
Fig. 10 The wall considered in the system's mode

Table 11 The comparison of quantitative results of an independent wall in mode of system with 45 degrees reinforcement armature

Row	Model's name	The maximum lateral load bearing capacity of a wall(N)	Increased lateral load bearing capacity of a wall compared to an independent wall
1	I-O-A45	29.500	0%
2	L-O-A45	35.746	21%
3	L-R-A45	58.359	98%
4	B-O-A45	48.048	63%
5	B-T-A45	48.000	63%
6	B-R-A45	62.008	110%

mode with asymmetrical load and given that this loading will create a twist in the structure, this increased load bearing will be 131 percent. It is noteworthy that adding roof to the panels will increase the load bearing capacity by 377%. The energy absorption of the structure in BOX shape mode in absence of twist will be increased by 150% but this increase will be 55% in case of existence of asymmetric load.

Reinforced wall with 45 degrees armatures have been considered as ideal walls. The capacity of one independent wall will be calculated after placement in a model after determination of its lateral capacity in order to have a more accurate evaluation of system's effect on three dimensional panel (Fig. 10).

The results of this analysis have been shown in Table 11. We conclude from the concluded analysis that independent wall with reinforced armature which will be in *L*-shape mode after connection to its vertical wall will have 21% increase in load bearing capacity. But this increase will not be so significant due to created twist, now, lateral load bearing capacity will be 2 times bigger by adding roof in order to remove twist effect which is considered to be a significant increase. Symmetrical load with 63% increase will be formed if a BOX system is formed with connection of independent wall to other three walls. This increased capacity will moment of inertia of structure due to connection of two walls perpendicular to the main wall at both ends. Also, the structure's symmetry will prevent the creation of additional twist which will prevent the reduction of lateral load capacity. Now, the lateral load bearing capacity of the independent wall will increase by 63% by having an asymmetric mode which means applying loading to one end of the wall (instead of both ends). It can be stated with evaluation of the total capacity of system and the wall that asymmetric load will decrease the total load bearing capacity of the system but no reduction can be
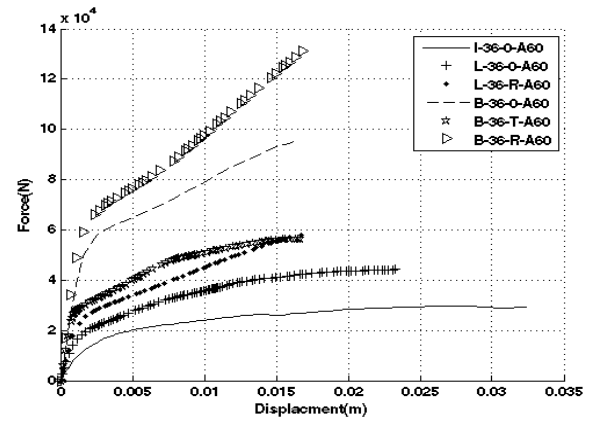

Fig. 11 The comparative additional load curve of panel with 60 degrees reinforcement armature

Table 12 The comparison of panel's quantitative results in six modes with 60 degrees reinforcement armature

Row	Model's name	The maximum load capacity (N)	Percent of increased bearing capacity	Energy absorption of the structures (N.m)	Percent of increased absorption Energy in the structure
1	I-O-A60	29.726	0%	805	0%
2	L-O-A60	44.303	49%	811	1%
3	L-R-A60	57.919	95%	671	-17%
4	B-O-A60	95.650	222%	1,178	46%
5	B-T-A60	56.463	90%	747	-7%
6	B-R-A60	131.334	342%	1,505	87%

observed in the capacity of evaluated wall and the capacity of other components of the system capacity will be reduced.

The increase in lateral load bearing capacity will be 110% higher than the independent wall in BOX shaped mode with wall which is due to the existence of rigid roof in free end of the wall.

5.5 Panel with 60 degrees reinforcement armature

Fig. 9 shows Fig. 11 shows the additional load comparative curve of Panel with 60 degrees reinforcement armature in 6 mentioned modes. The maximum lateral load capacity and energy absorption have been initially calculated for each model. Then, increase percentages of load capacity and energy absorption have been calculated compared to the independent wall. It can be concluded using the results of comparative Table 9 that improvement of behavior of the structure under the effect of 60 degrees reinforcement armature is similar to the existence of 45 degrees reinforcement armature in term of evaluating the lateral bearable load. In a way that this behavior improvements can be approved but energy absorption will reduce under *L*-shaped roofed performance which is due to reduced allowed displacement in *L*-shape mode, although there is no changes in energy absorption in *L*-shape mode without roof. The lateral load bearing capacity in 60 degrees reinforcement armature is similar to the existence of 45 degrees reinforcement armature in BOX shape mode but the

Table 13 The comparison of results between system's mode and independent mode

Row	Model's name	The maximum load capacity (N)	Percent of increased bearing capacity	Energy absorption of the structures (N.m)	Percent of increased absorption Energy in the structure
1	I-O-A00	15.500	0%	296	0%
2	I-O-A30	21.930	41%	587	98%
3	I-O-A45	29.500	90%	573	94%
4	I-O-A60	29.726	92%	805	172%
5	L-R-A00	21.572	0%	253	0%
6	L-R-A30	44.002	104%	597	136%
7	L-R-A45	62.331	189%	780	208%
8	L-R-A60	57.919	168%	671	165%
9	B-R-A00	49.886	0%	647	0%
10	B-R-A30	126.440	153%	1,991	208%
11	B-R-A45	140.858	182%	1,587	145%
12	B-R-A60	131.334	163%	1,505	133%

Table 14 The comparison of results between system's mode and independent mode

Row	model's name	K_i (kN/m)	Increase percentage of hardness of K_i	K_e (kN/m)	Increase percentage of hardness of Ke
1	I-O-A45	9500	0%	4200	0%
2	L-O-A45	19600	106%	11100	164%
3	L-R-A45	20800	119%	12000	186%
4	B-O-A45	37000	289%	22000	424%
5	B-T-A45	37500	295%	22200	429%
6	B-R-A45	49500	421%	30500	626%

Fig. 12 The comparison of hysteresis curve of independent wall and *L*-shaped wall with 45 degrees reinforcement armature

energy absorption of BOX shape mode with asymmetrical load will be reduced by 7% even compared to the independent wall which is due to reduced allowed movement. There are respectively 46% and 87% increased energy absorption in modes of symmetrical load and existence of roof. These values have been mentioned in Table 12.

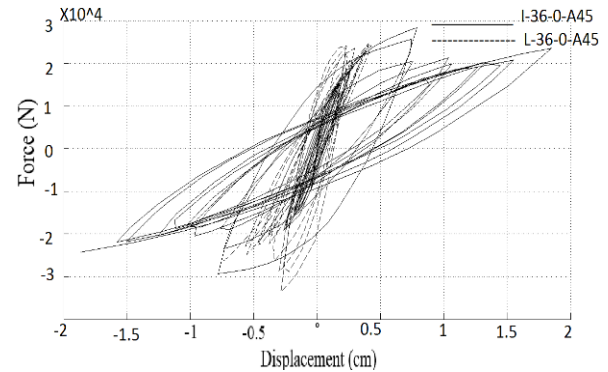### 5.6 Panel with the most optimal reinforcement armature

It can be concluded using comparative additional load curves in Figs. 7, 8, 9 and 11 as well as comparative Tables 8, 9, 10 and 11 obtained from analysis results of the independent wall, *L*-shape with roof and BOX shape with roof without reinforcement armature and with reinforcement armature with horizontal degrees of 30, 45 and 60 in all three modes that reinforcing the structure in independent mode with 45 and 60 degrees armature will have an almost identical behavior in terms of lateral load and of lateral load bearing capacity will be improved by about 90%.

Also armature with an angle of 30 degrees will provide 41% of load bearing capacity increase but the armature with 60 degrees has the best energy absorption in a way that it will lead to 172% increase. But 30 and 45 degrees armatures will lead to 95% increase. So reinforcement armatures with 60 degrees will have the best result in reinforcement of independent wall.

45 degree armatures will make the load bearing capacity 3 times higher and energy absorption 2.5 times higher in *L*-shape and BOX shape system modes but 30 degree armatures will make the load bearing capacity 2 to 2.5 times higher and energy absorption 2.5 times higher. Also 60 degree armatures will make the load bearing capacity 2.7 times higher and energy absorption 2.5 times higher. So using 45 degree reinforcement armatures will have the best result for reinforcement of walls in *L*-shape and BOX shape systems. These values have been mentioned in Table 13.

5.7 Panel comparing the hardness of the structures in system's mode

It can The hardness of Ki and Ke for structures without reinforcement armature and with 30, 45 and 60 degree reinforcement armature have been compared in table 14 for comparison of reinforcement armature's effect on three-dimensional independent panel walls according to which we observed the more proper hardness increase in use of 45 degrees reinforcement armature.

5.8 Armature comparing hysteresis curve

The amount of energy dissipation can be studied in this section with evaluation of hysteresis curve. Given that panels are ideal at the angle of 45 degrees, we will use their hysteresis curve for comparisons. Fig. 12 shows the comparison of hysteresis curve of independent wall and *L*-shaped wall with 45 degrees reinforcement armature. The independent wall will have more energy dissipation according to this figure. Fig. 13 shows the hysteresis curve of *L*-shaped wall and roofed *L*-shaped wall with 45 degrees reinforcement armature. It can be concluded based on this figure that *L*-shaped wall with roof is more depreciate. Fig. 14 shows the hysteresis curve of independent wall and roofed BOX shaped wall with symmetrical load without a roof. As predicted, BOX shaped wall with symmetrical loading will have a much higher energy depreciation than the independent Wall. Also Fig. 15 shows the comparison of hysteresis curve of BAX-shaped wall symmetrical and asymmetrical load. As can be seen, BOX shaped wall with
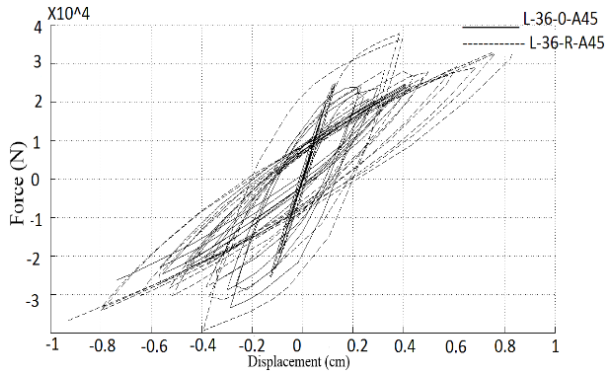
Fig. 13 The hysteresis curve of *L*-shaped wall and roofed *L*-shaped wall with 45 degrees reinforcement armature
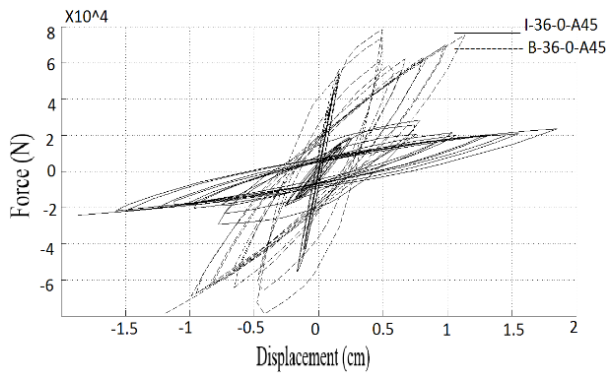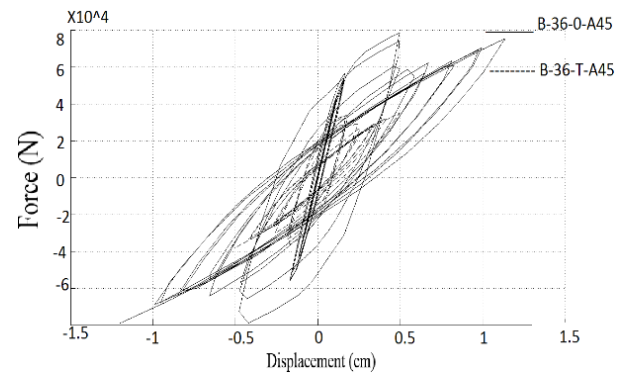

Fig. 15 The comparison of hysteresis curve of BOX-shaped wall symmetrical and asymmetrical load

Fig. 14 The hysteresis curve of independent wall and roofed BOX shaped wall with symmetrical load without a roof
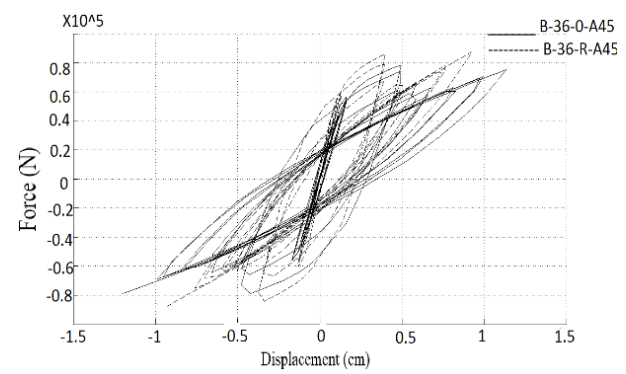

Fig. 16 The comparison of hysteresis curve between BOX-shaped walls with and without roof

symmetrical loading will have a higher energy dissipation compare *d* its similar structure with asymmetric load. The comparison of hysteresis curve between BOX-shaped walls with and without roof can be seen in Fig. 16. As can be seen, BOOX shaped wall with roof has a more spindle shaped diagram which shows a higher energy depreciation. It can concluded from the general comparison of hysteresis diagrams that *L*-shaped wall with twist caused by loading will have less energy depreciation compared to other models. It can also be stated that if a roof can lead to interrogated performance of wall, it can also increase energy depreciation but the roof will not lead to significant energy depreciation in symmetrical structures.

6. Conclusions

• In the *L*-shape wall without reinforcement armature, when the use of system effect is considered, this point should be noted that no twist due to geometry or loading should be

• In the *L*-shape wall without reinforcement armature, when the use of system effect is considered, this point should be noted that no twist due to geometry or loading should be allowed to happen in the structure. So, in the *L*-shape wall without the reinforcement armature, the lateral load capacity due to the twist has no significant difference with an independent wall. But when the roof is added to the structure, the lateral load capacity will increase about 40%

due to the reduction of the twist effect. But when 3-dimensional panel is reinforced by 10 mm ribbed armature, the lateral load capacity will increase even in the wall with twists. Approximately, in the *L*-shape wall without the roof, the lateral load bearing capacity will increase about 50% and in the *L*-shape wall with a roof, it will increase about 100%.

• In the BOX-shape wall, the wall reinforcement under the system effect will be very effective so that without the use of reinforcement armature, when the loading is symmetrical, the lateral loading capacity will have the increase of 200%. But when there is a twist in the structure due to the asymmetrical loading, the lateral load capacity will have an increase of 50%. If the panels are reinforced by angled reinforcement armatures, the lateral load capacity in symmetrical loading state, will be 3.5-4 times and in asymmetrical loading state, will be 2-2.5 times bigger.

• The more effective angle for reinforcement armature location in the independent wall is 45 and 60 degrees which will have 90 % increase in loading capacity. It can be said that the reinforced armature with the angle of 60 degrees will be slightly more effective than with the angle of 45. However, about the *L*-shape and BOX-shape walls, the use of the 45 degrees reinforcement armature will have the loading capacity increase of about 180%. For angles of 60 and 30, this increase will be 160 and 100%, respectively. Therefore to reinforce 3-dimensional panels, it is suggested to use the reinforcement armature with the angle of 45 degrees.

• To carefully study the effect of *L*-shape, once the lateral capacity of the independent wall was determined, the capacity of the same wall will be studied after locating in the *L*-shape and BOX-shape system. The results show that the independent wall with reinforcement armature which will be transformed to the *L*-shape state after connection to the vertical wall, will have the lateral loading capacity of 21% by own (not the whole system). But due to the existence of the twist, this capacity increase is a limited value. Now, by adding the roof to remove the effect of twisting, the lateral loading capacity will be two times more which is considered a significant increase. By connecting the independent wall to three other walls, if Box system is formed, in symmetrical loading, the increase of 63% will be related to the panel itself (not the whole system). By asymmetrical loading, i.e., applying the loading to the one end of the wall (instead of two walls), the lateral load capacity will have an increase of 50% compared to the independent wall but in comparison with the asymmetrical loading, will have 20% decrease in load capacity.

• Using 60 degrees reinforcement armature will have the most effective results to strengthen the independent wall.

• Using 45 degrees reinforcement armature will have the most effective results to strengthen the system mode walls which are *L*-shaped and BOX shaped walls.

• *L*-shaped wall which has the best twisted caused by loading has a low energy dissipation compared to other models. It can also be stated that if the existing roof causes an integrated performance, it can lead to energy dissipation but the roof will not lead to a significant increase in energy amortization in symmetrical structures.

References

Bassotti, O. and Ricci, M. (2002), "Caratteristiche di pannelli sandwich in cls. alleggerito e loro applicazioni costruttive", *Atti XIV Convegno CTE*, Mantova, 579-587.

Benayoune, A., Samad, A.A., Ali, A.A. and Trikha, D.N. (2007), "Response of pre-cast reinforced composite sandwich panels to axial loading", *Constr. Build. Mater.*, **21**(3), 677-685.

Benayoune, A., Samad, A.A., Trikha, D.N., Ali, A.A. and Ellinna, S.H.M. (2008), "Flexural behaviour of pre-cast concrete sandwich composite panel-experimental and theoretical investigations", *Constr. Build. Mater.*, **22**(4), 580-592.

Benayoune, A., Samad, A.A.A., Trikha, D.N., Ali, A.A.A. and Ashrabov, A.A. (2006), "Structural behaviour of eccentrically loaded precast sandwich panels", *Constr. Build. Mater.*, **20**(9), 713-724.

Buildings Design Code Resistant to Earthquake (2012), Standard No. 2800, Iissue 4, July, Iran. (in Persian)

Ceccoli, C., Mazzotti, C., Savoia, M., Dallavalle, G., Perazzini, G. and Tomassoni, F. (2002), "Indagine sperimentale su una tipologia di pannelli alleggeriti in ca gettati in opera", *Proceeding of Congress CTE*, Mantova, 7-9.

Einea, A., Salmon, D.C., Tadros, M.K. and Culp, T. (1994), "A new structurally and thermally efficient precast sandwich panel system", *PCI J.*, **39**(4), 90-101.

Fard, K.M. (2015), "Higher order static analysis of truncated conical sandwich panels with flexible cores", *Steel Compos. Struct.*, **19**(6), 1333-1354.

Foster, S.J. and Rogowsky, D.M. (1997), "Splitting of reinforced concrete panels under concentrated loads", *Struct. Eng. Mech.*, **5**(6), 803-815.

Gara, F., Ragni, L., Roia, D. and Dezi, L. (2012), "Experimental tests and numerical modelling of wall sandwich panels", *Eng. Struct.*, **37**, 193-204.

Giacchetti, R. and Menditto, G. (1984), "Indagini sperimentali su pannelli sandwiches realizzati con la tecnica dello spritzbeton", *Atti V Convegno CTE*, Firenze.

Kabir, M.Z. (2005), "Structural performance of 3-D sandwich panels under shear and flexural loading", *Scientia Iranica*, **12**(4), 402-408.

Kabir, M.Z. and Hasheminasab, M. (2002), "Mechanical properties of 3D wall panels under shear and flexural loading", *CSCE Conference*, 5-8.

Kabir, M.Z. and Vasheghani-Farahani, R. (2009), "Experimental investigation of performance in *L*-shaped wall to wall corner connections of 3D Panels subjected to lateral cyclic loading", *Struct. Eng. Mech.*, **33**(5), 649-652.

Kabir, M.Z., Jahanpour, A.R. and Rahbar, M.R. (2004), "An estimation of ductility and the behavior factor of 3D sandwich shotcreted panels subjected to monotonic shear loads", *High Performance Structures and Materials II*, 76-85.

Kabir, M.Z., Rezaifar, O. and Rahbar, M.R. (2007), "Upgrading flexural performance of prefabricated sandwich panels under vertical loading", *Struct. Eng. Mech.*, **26**(3), 277-295.

Numayr, K. and Haddad, R. (2009), "Static and dynamic analytical and experimental analysis of 3D reinforced concrete panels", *Struct. Eng. Mech.*, **32**(3), 399-406.

Pekelnicky, R. and Poland, C. (2012), "Seismic evaluation and retrofit of existing buildings", *SESOC Convention*.

Rezaifar, O., Kabir, M.Z., Taribakhsh, M. and Tehranian, A. (2008), "Dynamic behaviour of 3D-panel single-storey system using shaking table testing", *Eng. Struct.*, **30**(2), 318-337.

Salmon, D.C., Einea, A., Tadros, M.K. and Culp, T.D. (1997), "Full scale testing of precast concrete sandwich panels", *ACI Struct. J.*, **94**, 239-247.

Seeber, K.I.M.E., Andrews Jr, R.A.Y., Jacques, F.J., Baty, J.R., Kourajian, P., Campbell, P.S., ... and Paton, W. (1997), "State of the art of precast/prestressed sandwich wall panels", *PCI J.*, **42**(2), 92-133.

Sline, G. and Bush, T. (1994), "Flexural behavior of composite precast sandwich panels with continuous truss connectors", *PCI J.*, **39**(2), 112-121.

Strategic Supervision Department of Military Affairs (2012), *Three-Dimensional Prefabricated Panel System*, the First Revision, Publication No. 385. (in Persian)

CC